

Oral immunization with *Listeria monocytogenes* vaccine enhances immunotherapy for protective immunity in murine models of colorectal cancer

Xinyuan Lei,¹ Yangle Yu,¹ Charlie Chung,² Zhijuan Qiu,¹ Yue Zhang,¹ Timothy H Chu,¹ Xinran Li,¹ Rin Yang,¹ Khadir A Ozler,² Mami Burgac,² Peter M K Westcott,¹ Semir Beyaz,² Brian S Sheridan,¹

To cite: Lei X, Yu Y, Chung C, et al. Oral immunization with *Listeria monocytogenes* vaccine enhances immunotherapy for protective immunity in murine models of colorectal cancer. *Journal for ImmunoTherapy of Cancer* 2026;14:e011570. doi:10.1136/jitc-2025-011570.

► Additional supplemental material is published online only. To view, please visit the journal online (<https://doi.org/10.1136/jitc-2025-011570>).

XL and YY contributed equally.

Accepted 25 January 2026

ABSTRACT

Background Colorectal cancer (CRC) is a leading cause of cancer-related death and remains a significant global health challenge. Cancer vaccines have emerged as a promising immunotherapy for long-term tumor control. While *Listeria monocytogenes* (*Lm*)-based intravenous vaccines can generate tumor-reactive CD8 T cells, clinical trial success has been limited. Here, we sought to determine whether *in vivo* targeting of gastrointestinal tissues with foodborne delivery of *Lm*-based cancer vaccines controlled tumor growth in murine models of CRC.

Methods The ActA and InlB virulence genes were deleted from a mouse-adapted *Lm* strain expressing ovalbumin and containing an internalin A mutation (InlA^M*Lm*-ova) that allows epithelial cell invasion of mice to generate an oral vaccine administered via consumption of inoculated bread. Immunogenicity and safety were tested in C57BL/6 mice. Vaccine efficacy was evaluated with CRC tumors delivered by colonoscopy-guided orthotopic transplantation into the colon submucosa. Microsatellite instability high MC38 cell line expressing ovalbumin or genetically engineered microsatellite stable AKPS (*Apc*^{KO}*Kras*^{G12D}*Trp53*^{KO}*Smad4*^{KO}) organoids expressing low levels of ovalbumin (lo^{SIIN}) were used. Vaccines were tested in prophylactic and therapeutic settings and in the context of immune checkpoint inhibitors (ICI).

Results Oral immunization induced a robust CD8 T cell response that was similar in magnitude and phenotype to the fully virulent *Lm*. Immunized mice did not lose weight, and *Lm* was contained to intestinal tissues. Mice prophylactically immunized with the vaccine were protected from CRC tumors. Therapeutic immunization of mice bearing lo^{SIIN} AKPS tumors revealed curtailed growth of the local tumor but did not improve survival. Immunization with anti-programmed cell death protein-1 and anti-cytotoxic T-lymphocyte-associated protein 4 controlled tumors when coupled with therapeutic immunization. Protection correlated with accumulation of ova-specific CD8 T cells within the tumor.

Conclusions Oral *Lm*-based cancer vaccines targeting CRC elicit robust, widely disseminated, and persistent tumor-specific immune responses in mice. These vaccines limit CRC development when administered prophylactically and provide tumor control when administered

WHAT IS ALREADY KNOWN ON THIS TOPIC

⇒ *Listeria monocytogenes* (*Lm*) elicits potent innate and adaptive immune responses. Previous studies have demonstrated that intravenous delivery of *Lm*-based vaccines can generate tumor-reactive CD8 T cell responses. While there have been some successes, clinical trial results have often fallen short of expectations.

WHAT THIS STUDY ADDS

⇒ Oral immunization of highly attenuated *Lm* vaccine induces robust, widely disseminated T cell responses. Prophylactic vaccination of oral *Lm* vaccine also prevents colorectal cancer (CRC) development in multiple orthotopic CRC models. Therapeutic vaccination transiently curtailed CRC local growth in an aggressive CRC model that more closely mimics human CRC. Therapeutic vaccination with immune checkpoint inhibition controlled tumors.

HOW THIS STUDY MIGHT AFFECT RESEARCH, PRACTICE OR POLICY

⇒ Our findings underscore the potential of *Lm* as an oral cancer vaccine vector to target CRC. Additionally, prophylactic vaccination could be an effective measure to prevent CRC in high-risk populations, like Lynch syndrome.



© Author(s) (or their employer(s)) 2026. Re-use permitted under CC BY-NC. No commercial re-use. See rights and permissions. Published by BMJ Group.

¹Microbiology and Immunology, Stony Brook University Renaissance School of Medicine, Stony Brook, New York, USA
²Cold Spring Harbor Laboratory, Cold Spring Harbor, New York, USA

Correspondence to

Dr Brian S Sheridan;
 brian.sheridan@stonybrook.edu

Dr Semir Beyaz;
 beyaz@cshl.edu

therapeutically with ICI. Thus, oral delivery of *Lm*-based cancer vaccines coupled with ICI may provide improved control of CRC progression in clinical application.

BACKGROUND

Gastrointestinal (GI) cancers including colorectal cancer (CRC) represent a significant global public health challenge due to their high incidence and mortality rates.¹ Despite the widespread use of conventional therapies, there is a persistent concern regarding their inability to provide adequate long-term protection and their off-target effects on healthy tissues. The 5-year survival

rates, 64% for CRC,¹ underscore the pressing need for more effective and safer therapeutic approaches. Metastatic CRC, in particular, has a poor prognosis, with significantly lower survival rates. The tumor microenvironment (TME) plays a crucial role in cancer progression and response to therapies. Its immunosuppressive characteristics enable tumors to escape immune destruction.² Cancer immunotherapies have emerged as promising strategies to enhance antitumor immunity by overcoming immune tolerance and reversing TME-induced immunosuppression.³ However, GI cancers, especially microsatellite stable (MSS) and metastatic CRC respond poorly to existing immunotherapy modalities including immune checkpoint inhibitors (ICI) and chimeric antigen receptor-T therapy. Among developing immunotherapies, cancer vaccines have emerged as a promising strategy. They can educate the immune system to recognize cancer-related antigens in an *in vivo* setting that may enhance T cell targeting to tumor-bearing tissues by instructing appropriate homing molecules. In some contexts, they may also elicit antigen-independent mechanisms to overcome immunosuppression in the TME.^{3,4} Cancer vaccines appear a viable immunotherapy given the success of a recent phase I trial using a personalized messenger RNA neoantigen vaccine targeting pancreatic cancer.⁵

Among cancer vaccine approaches, live bacteria platforms stand out for their ability to stimulate robust antitumor immunity *in vivo* and potentially reshape the TME.⁶ *Listeria monocytogenes* (*Lm*), a gram-positive, intracellular bacterium, elicits potent innate and adaptive immune responses.⁷ On invading the intestinal epithelium via the surface protein internalin A (InLA), *Lm* uses the pore-forming listeriolysin O to escape into the cytosol from the phagosome. This escape mechanism allows *Lm* to engage in major histocompatibility complex (MHC) class I antigen presenting pathway, thereby triggering potent T cell responses. These responses are crucial for the sustained clearance of tumors.⁷ Additionally, *Lm* immunotherapy inhibits the immunosuppressive environment of the TME by reducing regulatory T cells (Treg) and myeloid-derived suppressor cells (MDSC)⁸ and promoting M1 macrophages.⁹ The ability to induce a potent T cell response, modulate the immune response within the TME, and induce cancer cell death through the generation of reactive oxygen species, makes *Lm* a compelling candidate for cancer vaccine vectors.¹⁰ Previous studies have also demonstrated that intravenous (i.v.) delivery of *Lm*-based vaccines can generate tumor-reactive CD8 T cell responses.¹¹ While there have been some successes,^{3,11,12} clinical trial results have often fallen short of expectations.^{13,14}

T cells are the primary mediators of antitumor immunity and play a central role in the response to immunotherapy. Tumors are often infiltrated by various numbers of immune cells.¹⁵ A multitude of studies across various cancer types, including CRC, consistently demonstrate a strong correlation between the presence of tumor-infiltrating CD8 T cells and

favorable outcomes, such as tumor regression and improved prognosis.¹⁶⁻¹⁸ Tissue resident memory T (T_{RM}) cells represent a subpopulation of memory T cells that reside in non-lymphoid tissues without recirculating and are phenotypically, functionally and transcriptionally distinct from circulating memory T cells.^{19,20} On re-exposure to antigen, T_{RM} cells are pre-positioned in the tissue to respond immediately and mediate protective immunity while the circulating T cells need to be recruited first, thus resulting in a delay in secondary immune response.^{21,22} T_{RM} cells express CD69 and the majority also express CD103.^{19,23} Tumor-infiltrating CD8 T cells that acquire a T_{RM} cell phenotype including the upregulation of CD103 are linked to enhanced cytotoxic T cell responses and better overall survival.^{24,25} Thus, the promotion of CD103⁺ T_{RM} cells emerges as a critical strategy for enhancing antitumoral immunity against GI cancers, emphasizing its significance in cancer vaccine design.²⁶

Despite promising therapeutic efficacy demonstrated in preclinical studies and clinical trials,^{3,5,6} challenges persist in optimizing *Lm*-based cancer vaccines for maximal effectiveness. Currently, most trials and preclinical work use i.v. delivery because the immunogenicity of highly attenuated oral *Lm* vaccines has been questionable.²⁷ To address this in mouse models, it is critical that a *Lm* strain capable of invading murine enterocytes is employed, as wild-type *Lm* is unable to invade these cells. Therefore, we established a murine model of *Lm* oral immunization using a recombinant strain of *Lm* with a mutation in the InLA (InLA^M) gene that facilitates interaction with murine E-cadherin to allow efficient invasion of mouse enterocytes similarly to how it occurs in humans.^{28,29} In the present study, we demonstrated that foodborne infection with InLA^M *Lm*-ova induced a significantly more robust ova-specific CD8 T cell response in the gut compared with i.v. infection, along with rapid accumulation of ova-specific CD103⁺ T_{RM} cells in the intestinal mucosa. The “murinized”, highly attenuated *Lm*-based cancer vaccines were highly immunogenic and safe after oral immunization. Prophylactic use of the oral *Lm*-based cancer vaccine prevented tumor development from orthotopic transplantation of the carcinogen-induced and microsatellite instability high (MSI) MC38 colon adenocarcinoma cell line in an antigen-specific manner. In addition, a similar antigen-specific restriction of tumor formation was observed after orthotopic transplantation of genetically engineered MSS *Apc*^{KO} *Kras*^{G12D} *Trp53*^{KO} *Smad4*^{KO} (AKPS) organoids that are designed to express low levels of the ova CD8 epitope SIINFEKL (lo^{SIIN} AKPS) to mimic normal neoantigen expression.³⁰ Administration of oral *Lm* vaccines initially limited the growth of established MSS lo^{SIIN} AKPS tumors but did not improve survival. However, *Lm* vaccination in combination with ICI led to profound tumor control that was associated with ova-specific CD8 T cell accumulation in the tumors.

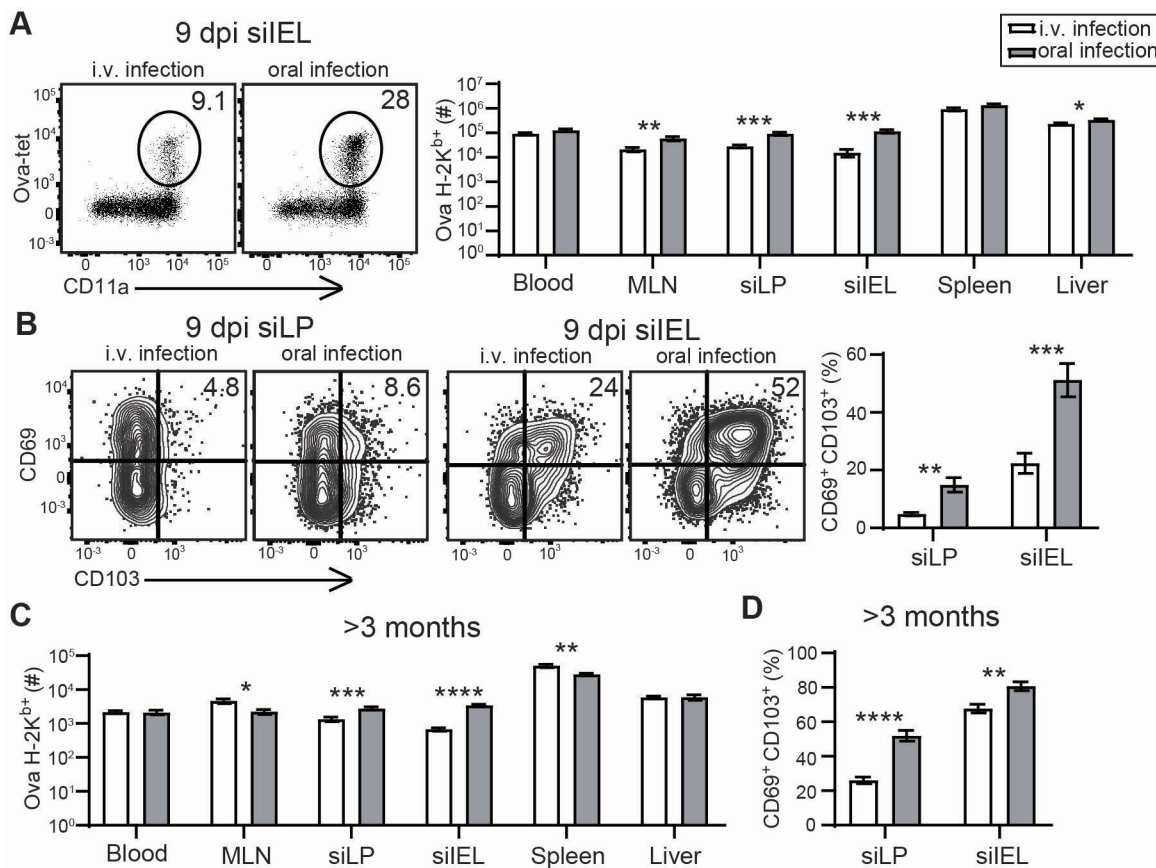


Figure 1 Foodborne infection induces superior intestinal CD8 T cell responses. B6 mice were administered 2×10^9 cfu of InLA^M *Lm*-ova by foodborne infection or 2×10^3 cfu of InLA^M *Lm*-ova by tail vein i.v. infection. (A) The absolute number of ova-specific T cells among CD8 α TCR β cells was determined with MHC I tetramers in the indicated tissues at 9 dpi. (B) Ova-specific CD8 T cells were assessed for CD69 and CD103 expression. (C) The absolute numbers of ova-specific CD8 T cells were quantified >3 months postinfection. (D) Ova-specific CD8 T cells were assessed for CD69 and CD103 expression. Cumulative data are shown from two independent experiments as mean \pm SEM with 9–11 mice/group. Representative flow plots are shown. *p<0.05; **p<0.01; ***p<0.001; ****p<0.0001 by Student's t-test. cfu, colony-forming units; dpi, days postinfection; InLA^M, mutation in the internalin A; i.v., intravenous; *Lm*, *Listeria monocytogenes*; MHC, major histocompatibility complex; MLN, mesenteric lymph node; siEL, small intestine intraepithelial lymphocyte; siLP, small intestine lamina propria; TCR β , T-cell receptor β .

Our findings underscore the potential of *Lm* as an oral cancer vaccine vector to enhance ICI responsiveness to CRC.

RESULTS

Foodborne infection promotes gut-focused T cell responses

C57Bl/6 (B6) mice were infected with 2×10^9 colony-forming units (cfu) of InLA^M *Lm*-ova by foodborne infection or 2×10^3 cfu of InLA^M *Lm*-ova by i.v. infection. Prior studies have determined that these doses lead to a similar internal burden of *Lm* in the liver and similar magnitude of circulating CD8 T cells.³¹ 9 days postinfection (dpi), foodborne infection induced a greater ova-specific CD8 T cell response in the mesenteric lymph nodes (MLN), small intestine lamina propria (siLP) and intraepithelial lymphocyte (siIEL) compartments, and liver. In contrast, the ova-specific CD8 T cell response was comparable in the blood and spleen (figure 1A). After foodborne infection, CD8 T cells rapidly upregulated CD69 and CD103 (figure 1B) demonstrating rapid acquisition of

a residency phenotype that did not occur after i.v. infection.³¹ Three months after infection, ova-specific CD8 T cells induced by foodborne infection were enriched in the siLP and siIEL (figure 1C) and maintained the more robust expression of CD103 (figure 1D). Conversely, ova-specific memory CD8 T cells were enriched in secondary lymphoid organs (MLN and spleen) after i.v. infection (figure 1C). These results suggest a potential benefit of an oral immunization strategy to target GI-focused cancers.

Oral immunization with *Lm* vaccines is immunogenic and safe

Lm-based vaccines need to be sufficiently attenuated for clinical use in patients with cancer. ActA enables *Lm*'s movement through the cytosol, promoting direct cell-to-cell dissemination while evading soluble mediators of immune control.³² InLB promotes *Lm*'s invasion of hepatocytes.^{33,34} Multiple attenuation strategies in a single vector ensure that a single reversion event will not lead to pathogenic vaccines. Deletion of these factors led to a 1,000-fold attenuation after intragastric administration of mice.³⁴ To evaluate oral *Lm* immunization on antitumor immunity,

we used the suicide-counterselection vector pLR16-Phes* to delete ActA and InlB sequentially from the InlA^M *Lm*-ova chromosome (Δ InlB Δ ActA InlA^M *Lm*-ova; online supplemental figure S1A).³⁵ The deletion of ActA and InlB was confirmed by colony PCR (online supplemental figure S1B) and sequencing (data not shown).

I.v. immunization with attenuated *Lm*-ova vaccines induces ova-specific CD8 T cells in mice.²⁸⁻³⁶ In our previous studies, foodborne infection with 2×10^9 cfu of the fully virulent InlA^M *Lm*-ova yielded a substantial gut-focused T cell response²¹⁻³¹ (figure 1 and online supplemental figure S2). However, highly attenuated *Lm* may be poorly immunogenic after oral administration as *Lm* needs to overcome the epithelial barrier for effective immunization. Hence, our objective was to determine the most appropriate dose of orally administered Δ InlB Δ ActA InlA^M *Lm*-ova that could elicit a comparable immune response to pathogenic InlA^M *Lm*-ova.

B6 mice were foodborne infected with 2×10^9 cfu of InlA^M *Lm*-ova or orally immunized with 2×10^9 , 2×10^{10} , or 2×10^{11} cfu of Δ InlB Δ ActA InlA^M *Lm*-ova. At the peak of the oral immune response (9 dpi),³⁷ Δ InlB Δ ActA InlA^M *Lm*-ova induced a diminished ova-specific CD8 T cell response compared with the pathogenic strain at the same dose. However, oral immunization with 2×10^{10} cfu elicited a similar magnitude ova-specific CD8 T cell response as the 2×10^9 cfu of virulent InlA^M *Lm*-ova at 7 dpi in blood, with similar results observed in ova-specific T cells at 9 dpi in MLN, siLP, siIEL, and spleen (online supplemental figure S3). Thus, a dose of 2×10^{10} cfu was used for subsequent experiments.

Despite the increased immunization dose, mice immunized with 2×10^{10} cfu of Δ InlB Δ ActA InlA^M *Lm*-ova did not lose weight (figure 2A) or show signs of diarrhea (data not shown). Additionally, we quantified replicative *Lm* in intestinal and extraintestinal tissues. As expected, bacterial burden in the small intestine was comparable between infected and immunized mice (figure 2B). However, there was a substantial decrease in *Lm* burden in the colon and MLN and *Lm* was essentially undetectable in extraintestinal tissues after oral immunization (figure 2B). Additionally, no pathological changes in gut tissues were observed (data not shown). Thus, a highly attenuated *Lm* vaccine was immunogenic and safe when administered orally.

Oral attenuated *Lm* vaccines induce normal CD8 T cell responses

We used adoptive transfer of OT-I cells to track the vaccine-elicited CD8 T cell response. 9 days after immunization, we evaluated the presence of OT-I cells in various tissues including MLN, siLP, siIEL, colon lamina propria (cLP), colon intraepithelial lymphocyte (cIEL), and spleen (figure 3A). Δ InlB Δ ActA InlA^M *Lm*-ova elicited a comparable OT-I T cell response as the fully virulent InlA^M *Lm*-ova in all evaluated tissues. Only a subtle but significant reduction was observed in siLP and cLP. Next, we assessed the phenotype of OT-I cells in each

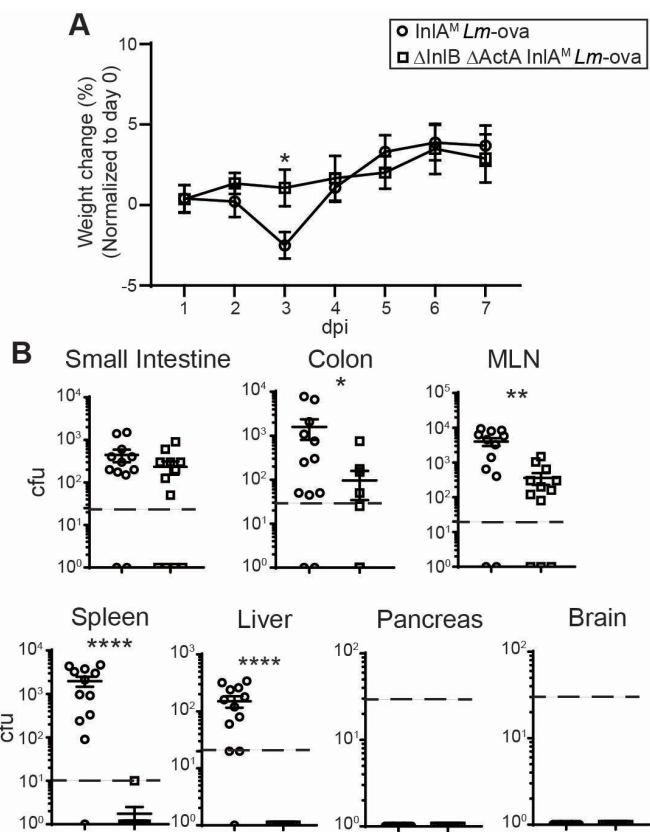


Figure 2 Safety profile of *Lm*-based cancer vaccines. B6 mice were orally administered 2×10^{10} cfu of Δ InlB Δ ActA InlA^M *Lm*-ova or 2×10^9 cfu of InlA^M *Lm*-ova. (A) Mice were weighed daily for 7 days. Cumulative data are shown from four independent experiments as mean \pm SEM with 8–11 mice/group. * $p<0.05$ by Student's t-test. (B) Bacterial burden was quantified 3 days postimmunization from the indicated tissues. The dashed line indicates the limit of detection for the assay from each tissue. Cumulative data are shown from three independent experiments as mean \pm SEM with 12 mice/group. ** $p<0.01$; *** $p<0.0001$ by Mann-Whitney test. cfu, colony-forming units; dpi, days postinfection; InlA^M, mutation in the internalin A; *Lm*, *Listeria monocytogenes*; MLN, mesenteric lymph node.

tissue to determine whether oral immunization with highly attenuated InlA^M *Lm*-ova altered T cell differentiation. Antigen-specific effector CD8 T cells that upregulate the interleukin (IL)-7 receptor α chain (CD127) represent memory precursor effector cells (MPEC; CD127⁺ KLRG1⁻). Conversely, cells expressing KLRG1 are more prone to undergo apoptosis during contraction and represent terminally differentiated short-lived effector cells (SLEC; KLRG1⁺ CD127⁻).³⁷ Our analysis revealed a similar differentiation pattern of MPEC in the MLN, siLP, siIEL, cLP, cIEL, and spleen (figure 3B). OT-I T cells in the gut formed similar or more T_{RM} precursor cells (CD69⁺ CD103⁺) after immunization (figure 3C). An assessment of endogenous ova-specific CD8 T cells revealed similar results in the MLN, siLP, siIEL, and spleen at 9 dpi (online supplemental figure S4). The functionality of vaccine-elicited T cells was also determined at 9 dpi. Cells were isolated from spleen, MLN,

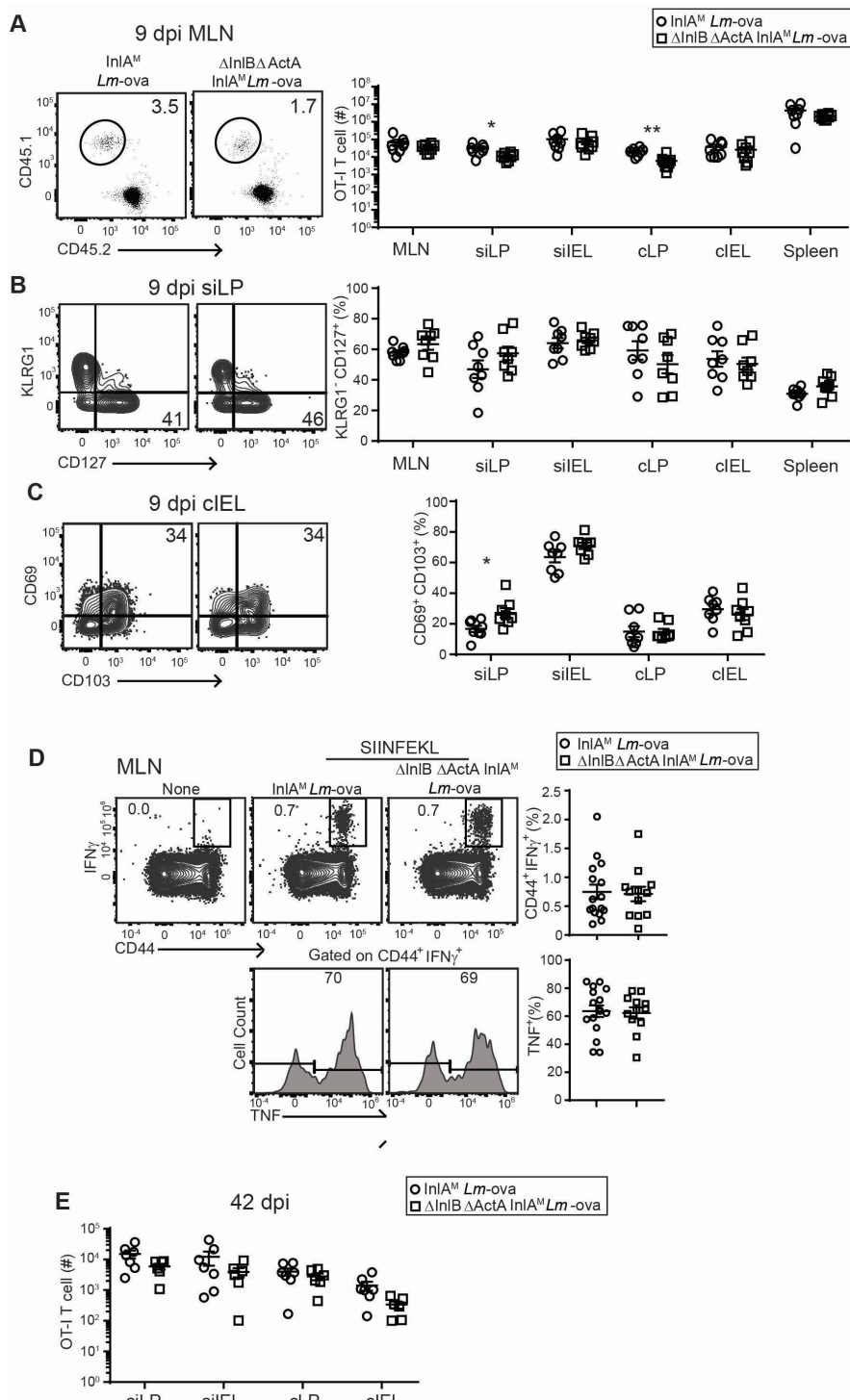


Figure 3 Highly attenuated *Lm* vaccine elicits robust CD8 T cells. (A–C, E) 1×10^4 splenocytes from a CD45.1⁺ OT-I TCR transgenic mouse were transferred into naïve CD45.2⁺ B6 mice. 1 day later, B6 mice were orally administered 2×10^{10} cfu of Δ InlB Δ ActA InlA^M *Lm*-ova or 2×10^9 cfu of InlA^M *Lm*-ova. (A) The absolute numbers of OT-I CD8 T cells were determined in the indicated tissues at 9 dpi. OT-I CD8 T cells were also assessed for CD127/KLRG1 (B) and CD69/CD103 (C) expression in the indicated tissues. (D) Naïve B6 mice were foodborne infected with 2×10^9 cfu of InlA^M *Lm*-ova or immunized with the 2×10^{10} cfu of Δ InlB Δ ActA InlA^M *Lm*-ova. 9 days postimmunization, cells from the MLN were isolated and stimulated with SIINFEKL peptide. IFN γ and TNF were assessed by intracellular cytokine staining. Cumulative data are shown as mean \pm SEM from four independent experiments with 13–15 mice/group. Representative flow plots are shown. (E) The absolute numbers of OT-I CD8 T cells were quantified at 42 days postimmunization. (A–C, E) Cumulative data are shown from two independent experiments as mean \pm SEM with 6–8 mice/group. Representative flow plots are shown. * p <0.05; ** p <0.01 by Student's t-test. cfu, colony-forming units; cIEL, colon intraepithelial lymphocyte; cLP, colon lamina propria; dpi, days postinfection; IFN γ , interferon-gamma; InlA^M, mutation in the internalin A; *Lm*, *Listeria monocytogenes*; MLN, mesenteric lymph node; siIEL, small intestine intraepithelial lymphocyte; siLP, small intestine lamina propria; TCR, T-cell receptor; TNF, tumor necrosis factor.

and siIEL and stimulated with the ova epitope to measure interferon-gamma (IFN γ) and tumor necrosis factor (TNF) production by intracellular staining. CD8 T cells were comparably functional after infection or immunization (figure 3D and online supplemental figure S5A and B). These data demonstrate that the vaccine elicits functional CD8 T cells. Furthermore, we assessed the induction and phenotype of memory OT-I cells in gut tissues at 42 dpi. The magnitude of the memory OT-I T cell response was comparable between immunized and infected mice in the intestines and colons (figure 3E). Additionally, while some variability in phenotype was observed, the expression of CD127 (online supplemental figure S5C) and CD69/CD103 (online supplemental figure S5D) was similar between the groups.

Next, we longitudinally assessed circulating OT-I cells. Despite a similar number of antigen-specific CD8 T cells in the tissues at 9 and 42 dpi, foodborne infection with 2×10^9 cfu of pathogenic InlA M *Lm*-ova resulted in a greater magnitude of circulating memory T cells, which emerged during contraction (figure 4A). Both groups of mice were then challenged by foodborne infection with 2×10^{10} cfu of pathogenic InlA M *Lm*-ova 43 days after initial immunization to assess the recall response. Mice immunized with *Lm*-vaccines displayed a robust recall response to the challenge infection that was comparable to mice that were initially infected with pathogenic *Lm* (figure 4A). At the time of challenge infection, most circulating T cells were of an MPEC phenotype. After challenge infection KLRG1 $^+$ cells rapidly emerged and dominated the recall response among both cohorts of mice (figure 4B), consistent with a conversion from a memory to an effector population. Secondary memory T cells were maintained comparably between immunized and infected cohorts. Responding antigen-specific CD8 T cells also demonstrated readiness for gut migration with increased expression of integrin $\alpha_4\beta_7$ (online supplemental figure S6A) and CXCR3 31 (online supplemental figure S6B).

We also evaluated the response of vaccine-elicited memory CD8 T cells to challenge infection in the tissues. The intestines and colons were isolated from *Lm*-immunized mice 7 days after challenge infection with 2×10^{10} cfu of pathogenic InlA M *Lm*-ova, a time that corresponded with the peak of the recall response in the blood (figure 4A). The magnitude of secondary effector T cells was similar between immunized and infected mice (figure 4C). Additionally, MPEC differentiation (figure 4D) and CD69 and CD103 expression (figure 4E) were comparable. OT-I cells were also examined 80 days postchallenge infection. Consistent with the primary memory response, immunization resulted in a similar secondary memory population as observed in mice infected with pathogenic *Lm* (online supplemental figure S7). Collectively, these findings demonstrate that oral immunization with highly attenuated *Lm* vaccines elicit normal CD8 T cell responses.

Oral *Lm* vaccines provide prophylactic control of CRC

We tested the efficacy of *Lm* vaccines in syngeneic CRC models using orthotopic transplant of MSI MC38-ova cell line by colonoscopy-guided injection into the colon submucosa.^{30 38 39} B6 mice were immunized with phosphate-buffered saline (PBS) (sham), 2×10^{10} cfu Δ InlB Δ ActA InlA M *Lm* (vector), or 2×10^{10} cfu Δ InlB Δ ActA InlA M *Lm*-ova (vaccine). 10 days postimmunization, mice were orthotopically transplanted with 1×10^6 MC38-ova cells, constitutively expressing ovalbumin. At 7 days post-tumor transplantation (dptt), tumor growth was visualized by colonoscopy to calculate tumor index (figure 5A). Tumor indexes span from 0 (no visible tumor) to 1 (complete obstruction). All mice from the sham and vector immunized groups developed CRC with tumor indexes mostly above 0.5, indicating substantial tumor growth. In contrast, 12 of 13 mice in the vaccinated group controlled tumor growth with no or minimal tumors detected at 7 dptt (figure 5B). Mice were euthanized at 8 dptt, and tumor weight and size were quantified. Tumors were undetectable from most vaccinated mice at 8 dptt (online supplemental figure S8). The magnitude of ova-specific T cells in circulation was notably higher in vaccinated mice but was still detectable in sham and vector-immunized mice. Furthermore, the differentiation of SLEC was either delayed or impaired in sham and vector immunized mice (figure 5C).

We also used the more aggressive and less immunogenic MSS lo SIIN AKPS organoid model for vaccine testing.³⁰ These organoids are derived from the normal mouse colon and engineered to harbor the most common cancer driver gene mutations observed in metastatic human MSS CRC. The use of organoids more accurately recapitulates the histopathological progression and complex tumor environment of human disease. Additionally, low expression of neoantigen, rather than a complete absence of neoantigens, better mimics the typical tumor antigen expression profile of MSS CRC in humans.^{30 40 41} 10 days postimmunization, 1×10^6 cell-worth of MSS lo SIIN -GFP AKPS organoids were orthotopically injected into colon submucosa of GFP-tolerized recipient mice by optical colonoscopy for further evaluation (figure 5D). Orthotopic transplant of lo SIIN AKPS leads to approximately 50% metastasis and animal death beginning around 40 dptt.³⁰ Vaccinated mice restricted lo SIIN AKPS tumor growth. In contrast, the sham-immunized mice exhibited significant tumor growth (figure 5E). While the magnitude of ova-specific CD8 T cells in circulation was comparable between sham and immunized mice, protection was associated with the development of a pronounced SLEC phenotype (figure 5F). Collectively, these data demonstrate that protection against CRC development is associated with SLEC differentiation of antigen-specific CD8 T cells.

Therapeutic oral vaccination curtails local growth of CRC

We proceeded to evaluate the therapeutic efficacy of oral *Lm* vaccines with the MSS lo SIIN AKPS organoid

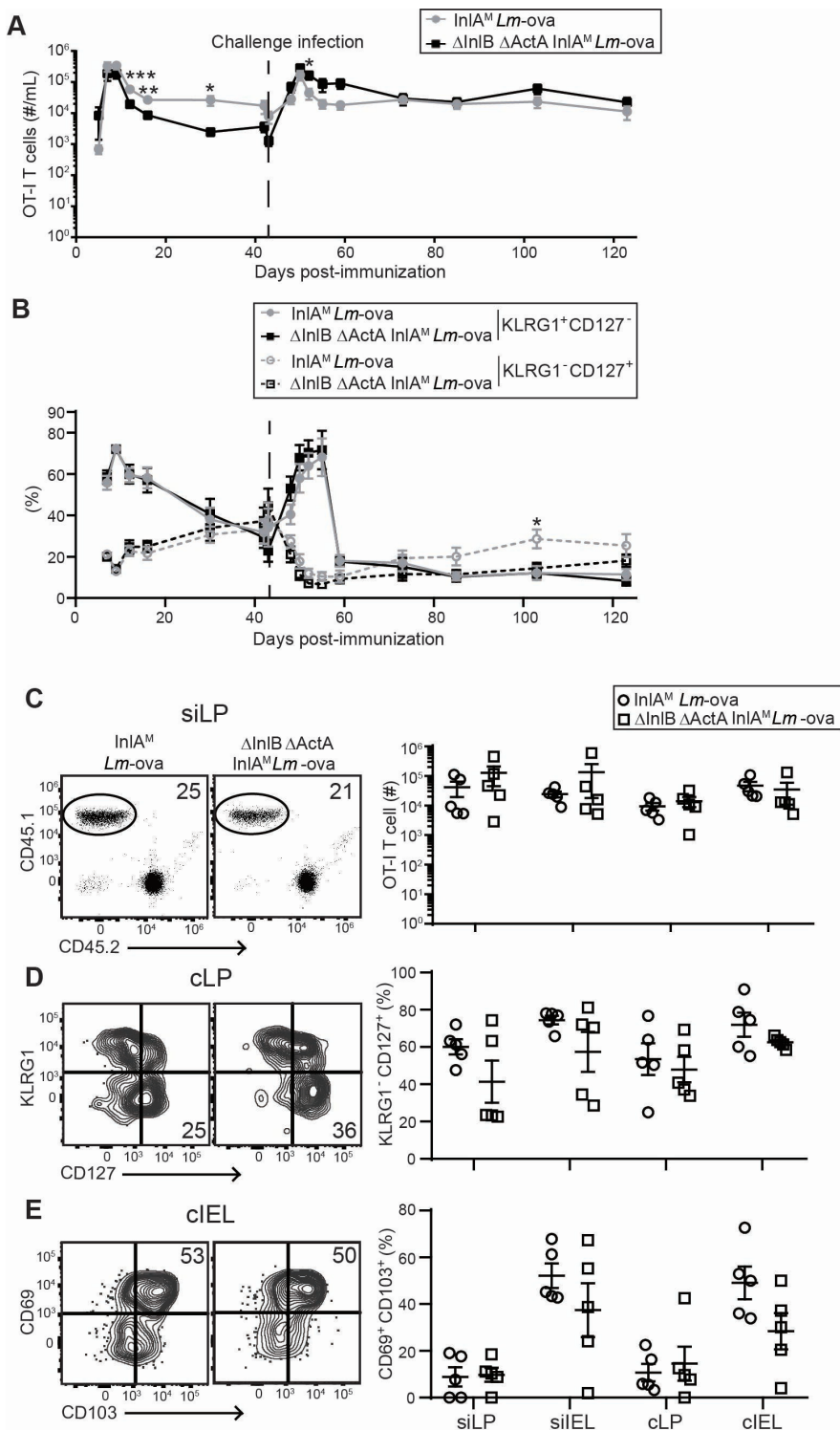


Figure 4 Challenge with pathogenic *Lm* elicits recall of vaccine-induced memory cells. 1×10^4 splenocytes from a CD45.1⁺ OT-I TCR transgenic mouse were transferred into naïve CD45.2⁺ B6 mice. 1 day later, B6 mice were orally administered 2×10^{10} cfu of Δ InlB ΔActA InlA^M *Lm*-ova or 2×10^9 cfu of InlA^M *Lm*-ova. 43 days after immunization (vertical dashed line), mice were challenged with 2×10^{10} cfu of InlA^M *Lm*-ova by foodborne infection. (A) The number of OT-I T cells was longitudinally determined in the blood at the indicated times postimmunization. (B) CD127 and KLRG1 expression of OT-I T cells was assessed at the indicated times. Cumulative data are shown from six independent experiments as mean \pm SEM with 4–19 mice/time point. * p <0.05; ** p <0.01; *** p <0.001 by Student's t-test. (C) The number of OT-I cells was determined by flow cytometry in the indicated tissues 7 days after challenge infection. OT-I cells were also assessed for CD127/KLRG1 (D) and CD69/CD103 (E) expression. Cumulative data are shown from two independent experiments as mean \pm SEM with 4–5 mice/group. Representative flow plots are shown. cfu, colony-forming units; cIEL, colon intraepithelial lymphocyte; cLP, colon lamina propria; dpi, days postinfection; InlA^M, mutation in the internalin A; *Lm*, *Listeria monocytogenes*; siEL, small intestine intraepithelial lymphocyte; siLP, small intestine lamina propria; TCR, T-cell receptor.

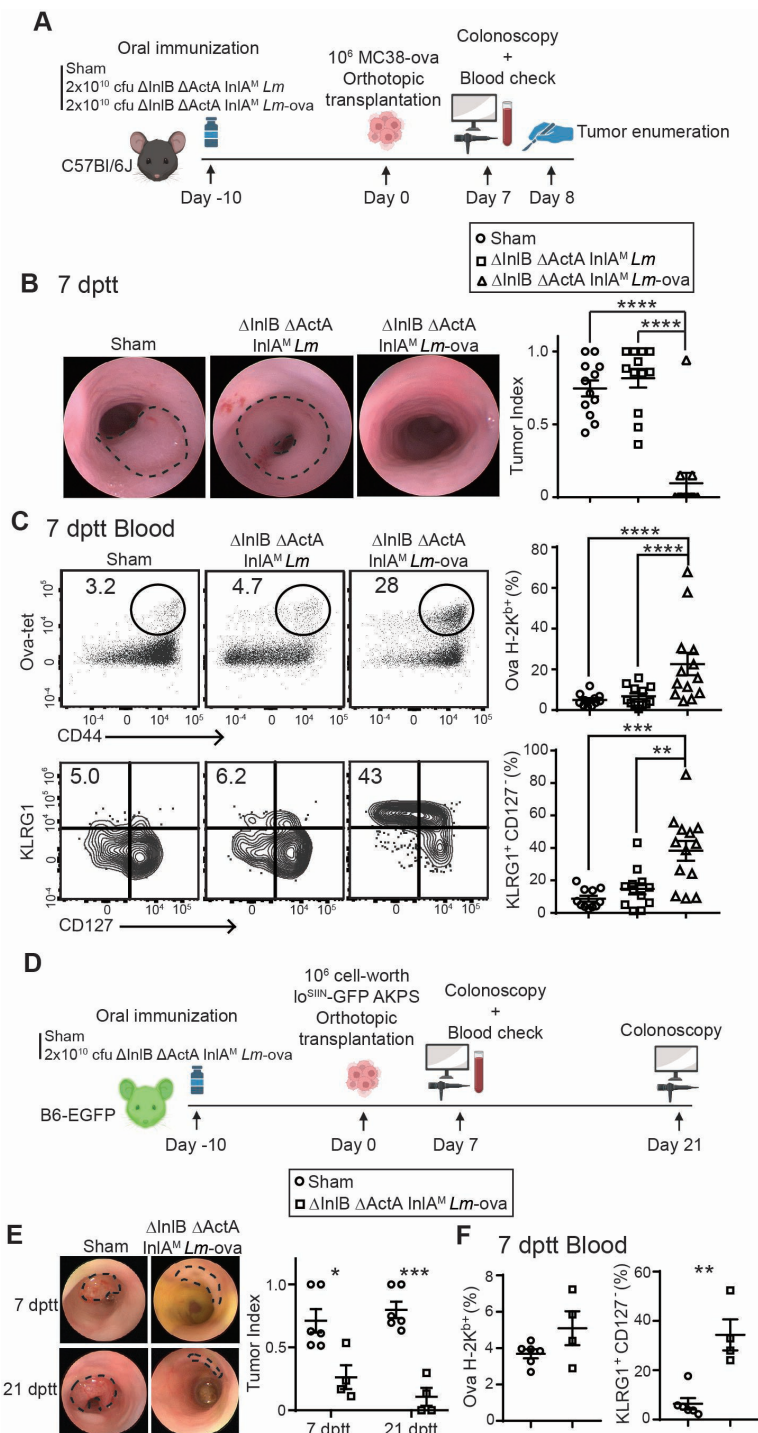


Figure 5 Oral *Lm* vaccines control CRC. Naïve B6 mice were orally immunized with the 2×10^{10} cfu of Δ InlB Δ ActA InlA^M *Lm*, 2×10^{10} cfu of Δ InlB Δ ActA InlA^M *Lm*-ova or PBS. 10 days later, 1×10^6 MC38-ova cells were orthotopically transplanted into colon submucosa by optical colonoscopy. Tumors were measured by colonoscopy at 7 dptt. (A) Schematic depiction of experimental outline of prophylactic immunization and MC38-ova transplant. (B) Ova-specific T cells were identified among CD8 α TCR β cells. KLRG1 and CD127 were assessed among ova-specific CD8 T cells. (AC) Cumulative data are shown from two independent experiments as mean \pm SEM with n=12–13 mice/group. Representative flow plots are shown. **p<0.01; ***p<0.001; ****p<0.0001 by one-way ANOVA with a post-hoc Tukey's multiple comparisons test. Naïve B6-EGFP mice were orally immunized as above. 10 days later, 1×10^6 cells-worth of organoids were orthotopically transplanted into colon sub-mucosa of B6-EGFP mice by optical colonoscopy. (D) Schematic depiction of experimental outline for prophylactic immunization with *lo*^{SIN} AKPS transplant. (E) Colonoscopy was performed at 7 and 21 dptt. (F) Ova-specific T cells were identified among CD8 α TCR β cells. KLRG1 and CD127 were assessed among ova-specific CD8 T cells. Cumulative data are shown from two independent experiments as mean \pm SEM with 4–6 mice/group. *p<0.05; **p<0.01; ***p<0.001 by Student's t-test. ANOVA, analysis of variance; cfu, colony-forming units; CRC, colorectal cancer; dptt, days post-tumor transplantation; InlA^M, mutation in the internalin A; *Lm*, *Listeria monocytogenes*; PBS, phosphate-buffered saline; TCR, T-cell receptor.

orthotopic model. 7 days after orthotopic transplant, colonoscopy was performed to measure baseline tumor growth. Mice were subsequently sham immunized or immunized with the vector or vaccine. 28 days

postimmunization, mice were boosted with their initial immunization regimen. A colonoscopy was performed 14 days after primary immunization and 7 days post-boosting to visualize tumor growth (figure 6A). Sham and vector

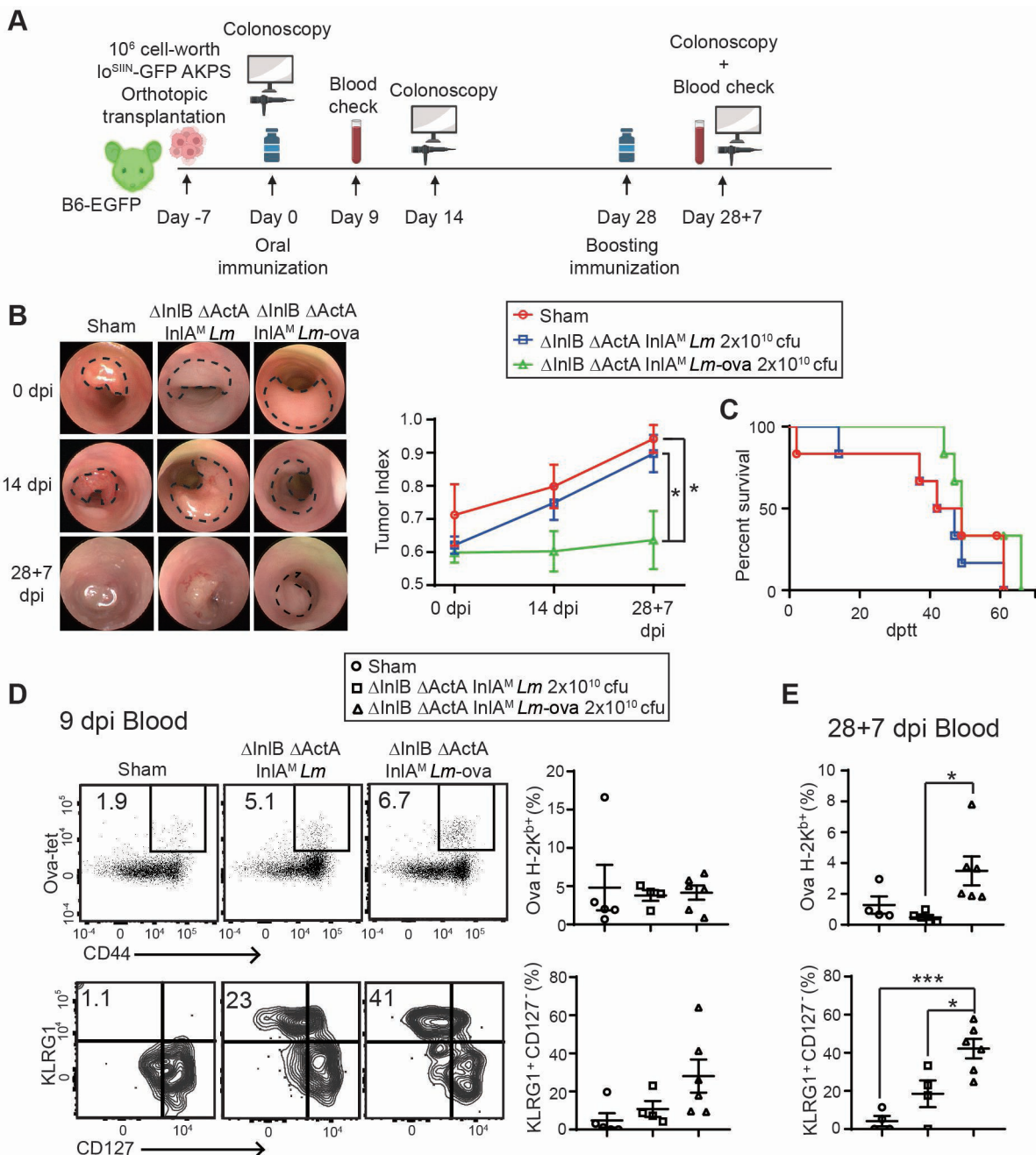


Figure 6 Therapeutic vaccination transiently limits tumor growth. Naïve B6-EGFP mice were orthotopically transplanted with 1×10^6 cell-worth of organoids into the colon submucosa by optical colonoscopy. Tumors were measured by colonoscopy 7 days later. Mice were subsequently orally immunized with 2×10^{10} cfu of Δ InlB Δ ActA Δ InlB Δ ActA, 2×10^{10} cfu of Δ InlB Δ ActA Δ InlB Δ ActA, or PBS. 28 days post primary immunization, mice were boosted with their initial immunization regimen. (A) Schematic depiction of experimental outline for therapeutic immunization of mice bearing *Io*^{SIN} AKPS tumors. (B) 7 days post-boosting, tumors were measured by colonoscopy. (C) Kaplan-Meier survival curves of the mice in each group (dptt, days post-tumor transplant). 9 days post primary immunization (D) and 7 days post boosting (E), ova-specific T cells were identified among CD8^a TCR β cells. KLRG1 and CD127 were assessed among ova-specific CD8 T cells. Cumulative data are shown from two independent experiments as mean \pm SEM with 6 mice/group. Representative flow plots are shown. *p<0.05; ***p<0.001 by one-way ANOVA with a post hoc Tukey's multiple comparisons test. ANOVA, analysis of variance; cfu, colony-forming units; dpi, days postinfection; dptt, days post-tumor transplantation; InlA^M, mutation in the internalin A; *Lm*, *Listeria monocytogenes*; PBS, phosphate-buffered saline.

immunized mice were unable to control tumor growth in the colon. In contrast, vaccinated mice initially controlled tumor growth but rapidly succumbed similarly to sham or vector immunized mice (figure 6B and C). Circulating ova-specific CD8 T cells were assessed 9 days after initial immunization and 7 days after boosting. At 9 days postimmunization, the magnitude and phenotype of circulating ova-specific T cells were similar in each group (figure 6D). However, by 7 days after boosting, an increased ova-specific T cell response was detected in the blood of mice boosted with Δ InlB Δ ActA InlA^M *Lm*-ova. This enhanced T cell response was associated with the emergence of a pronounced SLEC phenotype (figure 6E). To further determine whether the transient control of Δ InlB Δ ActA InlA^M *Lm*-ova against tumor is driven by an antigen-specific CD8 T cell response induced by oral *Lm* vaccines, we orthotopically transplanted MSS AKPS organoids that lack SIINFEKL expression (no^{SIIN}) into mice who were subsequently immunized and boosted with *Lm*-ova vaccines. Colonoscopy performed 7 days after boosting revealed that *Lm*-ova immunization failed to control the growth of AKPS tumors that lack SIINFEKL expression despite substantial accumulation of ova-specific CD8 T cells in the tumors (figure 7A and B). Thus, therapeutic immunization with antigen-expressing *Lm* vaccines can drive a tumor-reactive CD8 T cell response that provides transient control of tumor growth.

Since oral *Lm*-ova vaccines only transiently controlled lo^{SIIN} AKPS tumors, we reasoned that the transient nature of tumor control may be due to immune checkpoints after induction of the CD8 T cell response. Therefore, we evaluated the therapeutic efficacy of combining *Lm*-ova vaccines with ICI. Starting 5 days after primary immunization, lo^{SIIN} AKPS tumor-bearing mice were treated with ICI therapy (anti-programmed cell death protein-1 (PD-1) and anti-cytotoxic T-lymphocyte-associated protein 4 (CTLA4)) every other day for 2 weeks. A colonoscopy was performed 7 days after organoid transplantation and 7 days after vaccine boosting. The combinatorial administration of *Lm* vaccines and ICI therapy markedly suppressed the growth of tumors compared with either therapy alone (figure 7C). Consistent with previous findings, lo^{SIIN} AKPS tumors were poorly responsive to anti-PD-1 and anti-CTLA4 therapy,³⁰ while *Lm*-ova vaccines substantially enhanced the sensitivity of lo^{SIIN} tumors to ICI therapy. Circulating ova-specific CD8 T cells increased in both vaccine alone and vaccine plus ICI groups (figure 7D). Notably, only *Lm*-ova vaccines in combination with ICI significantly promoted the accumulation of ova-specific CD8 T cells within tumors (figure 7E). Altogether, these results demonstrate that oral *Lm* vaccines can improve the therapeutic efficacy of ICI therapy in poorly responsive tumors by driving tumor accumulation of antigen-specific CD8 T cells.

DISCUSSION

Cancer immunotherapy represents a treatment strategy that harnesses a person's own immune system to combat

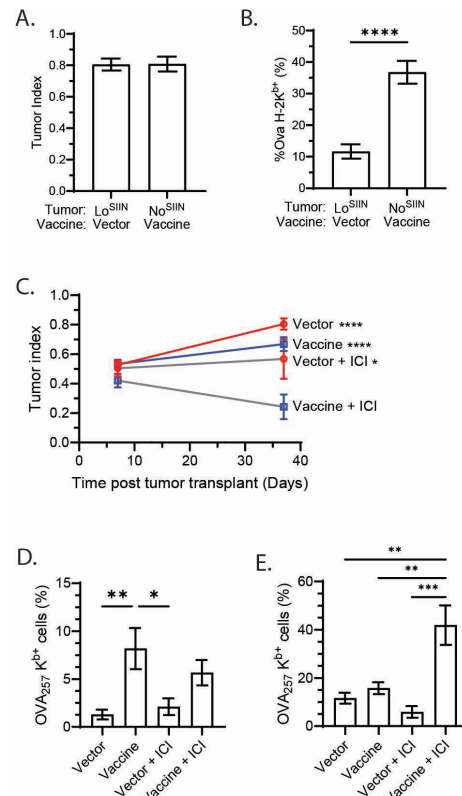


Figure 7 Oral *Lm* vaccines enhance tumor response to ICI therapy. (A–B) Naïve B6-EGFP mice were orthotopically transplanted with 0.5×10^6 cell-worth of lo^{SIIN} AKPS or no^{SIIN} AKPS organoids into the colon submucosa by optical colonoscopy. Mice were subsequently orally immunized with 2×10^{10} cfu of Δ InlB Δ ActA InlA^M *Lm* (vector) or Δ InlB Δ ActA InlA^M *Lm*-ova (vaccine) as indicated. On 23 days post-primary immunization, mice were boosted with their initial immunization regimen. (A) Colonoscopy was performed at 37 dptt. (B) Ova-specific T cells were identified among CD8 α TCR β cells within tumors at 37 dptt. (C–E) Naïve B6-EGFP mice were orthotopically transplanted with 0.5×10^6 cell-worth of lo^{SIIN} AKPS organoids into the colon submucosa by optical colonoscopy. Tumors were measured by colonoscopy 7 days later. Mice were subsequently orally immunized with 2×10^{10} cfu of Δ InlB Δ ActA InlA^M *Lm* (vector) or Δ InlB Δ ActA InlA^M *Lm*-ova (vaccine). On 5 days postimmunization, mice were intraperitoneally injected with anti-PD-1 antibody and anti-CTLA-4 antibody every other day for 2 weeks (ICI). On 23 days post-primary immunization, mice were boosted with their initial immunization regimen. (C) Colonoscopy was performed at 7 and 37 dptt. Statistics are shown for all groups versus Vaccine+ICI group. (D) Circulating ova-specific T cells were identified among CD8 α TCR β cells at 37 dptt. (E) Ova-specific T cells were identified among CD8 α TCR β cells within tumors at 37 dptt. Cumulative data are shown from three independent experiments as mean \pm SEM with 7–16 mice/group. * p <0.05; ** p <0.01; *** p <0.001, **** p <0.0001 by a Student's t-test (B) or one-way ANOVA with a post hoc Tukey's multiple comparisons test (C–E). ANOVA, analysis of variance; cfu, colony-forming units; CTLA-4, cytotoxic T-lymphocyte-associated protein 4; dptt, days post-tumor transplantation; ICI, immune checkpoint inhibitor; InlA^M, mutation in the internalin A; *Lm*, *Listeria monocytogenes*; PD-1, programmed cell death protein-1; TCR, T-cell receptor.

cancer. Unlike traditional treatments such as invasive surgery, chemotherapy, and radiotherapy, which can cause significant collateral damage to the body, immunotherapy has the capacity to provide more persistent, targeted cancer clearance and long-term surveillance. In this context, cancer vaccines have emerged as a promising avenue for immunotherapy, offering the potential to eradicate tumors while establishing durable antitumor immunity. A critical consideration for any replicating vaccine is its safety profile, particularly for immunocompromised individuals such as patients with cancer. Extensive clinical trials using i.v. infusion of 1×10^8 – 1×10^9 cfu of attenuated *Lm* have established a generally manageable safety profile, characterized by common, self-limiting events like fever, chills, and nausea.⁴² Current protocols include post-*Lm* administration of antibiotics to limit adverse events. Despite this, rare, serious adverse events like listeriosis and septic shock have been reported.^{12,43,44} Oral immunization with highly attenuated *Lm* vaccines has rarely been explored due to concerns about their ability to cross the epithelial barrier and elicit strong immune responses. A Phase I clinical trial demonstrated the safety of an orally administered, highly attenuated *Lm* influenza vaccine. Although no influenza antigen-specific immune responses were observed, anti-*Lm* responses were detectable suggesting immunogenicity is obtainable.²⁷ In our study, we used a “murinized” *Lm* strain lacking the ActA and InlB virulence factors, limiting bacterial infection to epithelial and phagocytic cells. The murinized strain of *Lm* invades the intestines through InlA-dependent (eg, through intestinal epithelial cells) and InlA-independent mechanisms (eg, through Microfold cells).^{28,45} Dissemination to the MLN is primarily mediated by carriage in dendritic cells through afferent lymphatics. Once there, *Lm* divides extensively in Batf3-dependent cDC1 cells, which are also critical for induction of the antigen-specific CD8 T cell response.⁴⁶ With a dose only one log higher than the pathogenic strain, we observed a robust and widely disseminated antigen-specific CD8 T cell response after immunization. A reduction or absence of replicative *Lm* in the colon, MLN, spleen, liver, pancreas, and brain confirmed the safety profile of this approach. The tissues were selected based on their relevance as potential target organs for cancer vaccine therapies (eg, primary tumor development in pancreas and colon; common metastasis sites in MLN, liver, and brain) or their association with listeriosis (liver and brain). Interestingly, there was an approximate 90% reduction in bacteria isolated from the colon which may be due to a reported role of ActA in promoting bacterial aggregation and survival in the gut lumen⁴⁷ or InlB in promoting *Lm* transmigration through intestinal epithelial cells.⁴⁸ The oral immunization route explored in this study may also offer a superior safety advantage to i.v.-based *Lm* vaccines. The primary risk of i.v. platforms is the inherent systemic bacterial exposure. In contrast, our model demonstrated limited systemic dissemination following oral immunization, suggesting that a mucosal delivery route could significantly reduce

the risks of bacteremia and systemic toxicity in patients, thereby representing a promising and safer alternative for vulnerable patient populations.

The TME plays a crucial role in cancer progression and response to treatment. It is inherently immunosuppressive, employing various mechanisms such as overexpression of inhibitory receptors like programmed death-ligand 1 (PD-L1), downregulation or loss of tumor antigens, shedding of soluble MHC I, and release of immunosuppressive molecules like IL-10 and transforming growth factor β .⁴⁹ These mechanisms collectively shape the TME, allowing transformed cells to evade immune surveillance during the elimination phase, leading to uncontrolled growth and metastasis.⁴⁹ Within the TME, CD8 T cells often undergo progressive loss of effector functions such as the production of effector cytokines and cytolytic molecules. This dysfunctional state is known as T cell exhaustion and is associated with lack of tumor control.⁵⁰ *Listeria* vaccines have the potential to reshape TME while boosting the generation of robust, widely disseminated, long-lived tumor-specific T cells. Foodborne infection elicits more gut-focused antigen-specific T_{RM} cells while i.v. infection elicits more antigen-specific T cells in the circulation. An oral vaccine system may be more beneficial for control of tumors that require gut-tropic T cells for protection such as colorectal, small intestine, or pancreatic cancers, where the primary tumor site is within the GI system. Alternatively, i.v. administration might better target broadly disseminated tumors. The ability to differentially target T cells to distinct compartments via route of immunization may provide great utility for tailoring immunization strategies to target solid tumors of various tissues or those that have broadly disseminated after metastasis. However, more work needs to assess the impact of priming on anti-tumor response elicited by vaccination and ICI in distinct tumor-bearing tissues. Recent evidence has linked a TCF1⁺ PD-1⁺ CD8 T cell population with ICI responsiveness and positive outcomes after neoantigen vaccination with a TLR7/8 agonist.⁵¹ Similar populations of progenitor-like CD8 T_{RM} cells in the intestines have been described.⁵² *Lm* also possesses the unique ability to directly infect cells and remain intracellular while spreading, enabling *Lm* to evade humoral immunity and making repeated administrations to boost immune function feasible.⁵³ The flexibility in boosting allows for the utilization of different routes of immunization to tailor the immune response to the patient’s needs.⁶

Cancer prevention encompasses a diverse range of approaches including chemoprevention, surgery, behavioral science interventions, and vaccines.⁵⁴ A *Listeria*-based oral cancer vaccine provides a potential avenue for prophylactic immunization targeting tumor antigens for individuals at high risk of GI-focused cancers. Indeed, oral immunization with highly attenuated Δ InlB Δ ActA InlA^M *Lm* vaccines has demonstrated prophylactic efficacy against MC38 and AKPS organoid tumors in an antigen-specific manner. While the MC-38 syngeneic model has been studied extensively in prophylactic models, most

studies reported delayed tumor growth and prolonged survival,^{55 56} complete rejection has rarely been reported, and often used subcutaneous tumor implantation. Regardless of the cancer model, tumor development was prevented or eliminated in almost all animals as early as seven dptt in our study. Protection from tumor development was associated with a greater ova-specific T cell response and a terminally differentiated phenotype. Ova-specific CD8 T cells induced by tumors in the absence of immunization displayed compromised expansion and differentiation, consistent with previous findings.³⁰ These ova-specific T cells were unable to initially control tumor growth. These findings provide strong evidence of effective prophylactic control of aggressive orthotopic CRC models that may be beneficial for high-risk CRC populations. For example, individuals with Lynch syndrome might benefit from prophylactic immunization.^{57 58}

Ova-specific CD8 T cells induced by MSI MC38-ova without immunization ultimately eliminated tumors (data not shown), making MSI MC38-ova an insufficient model to evaluate therapeutic vaccination. We used the more aggressive and less immunogenic MSS lo^{SIIN} AKPS organoid model for therapeutic vaccine testing since it also better mimics human CRC.³⁰ In this model, oral immunization with the *Lm* cancer vaccine after tumor development curtailed local tumor growth. Control of local tumor growth was associated with a more robust antigen-specific T cell response and a terminally differentiated phenotype. However, even though tumor growth was transiently controlled, the tumors were not eliminated, which may lead to treatment failure and metastases. In the absence of elimination, the vaccine-elicited tumor-reactive T cells may become suppressed. Multiple underlying causes may contribute to the emergence of immune evasion. For example, expression of immune checkpoint ligands, such as PD-L1, that subvert T cell effector functions in the tumor and increased numbers of Treg cells and MDSC may be emerging to prevent tumor elimination.⁵⁹ Indeed, combinatorial therapy with vaccination and ICI reduced tumor burden considerably and most mice had barely detectable tumors at the study endpoint.

A subpopulation of CRC accumulates a high frequency of somatic mutations resulting in enhanced neoantigen presentation,⁶⁰ which is referred to as microsatellite instability and may be predictive of ICI responsiveness in metastatic CRC.⁶¹ However, most patients with CRC, who are MSS, like the AKPS organoids employed in this research, are refractory to the original Food and Drug Administration-approved ICI immunotherapies, especially in advanced stages of disease. Our research demonstrates the potential for oral *Lm*-based cancer vaccines to target CRC and enhance tumor responsiveness to ICI therapy. This vaccine uses various approaches to target GI tumors including using highly attenuated live bacteria, oral immunization, and an antigen expression system that closely mimics bona fide tumor-associated antigen expression levels.⁶² Presently, only a limited number of

therapeutic vaccines have demonstrated clinical efficacy.⁶³ Multiple underlying causes may contribute to the lack of positive clinical outcomes in many trials that may necessitate employing multiple modalities to overcome. In the context of advanced tumors, therapeutic approaches often involve tumor debulking through surgery, chemotherapy, or radiotherapy.⁶⁴ In this context, therapeutic vaccinations aimed at diminishing the number of residual cancer cells may also promote immunological memory that could aid in limiting tumor recurrence.

MATERIAL AND METHODS

Bacteria and vaccines generation

Lm strain 10 403s carrying two amino acid changes in the InLA protein and expressing truncated ovalbumin (InLA^M *Lm*-ova) was used.^{65 66} The truncated ovalbumin contains the SIINFEKL CD8 T cell epitope but lacks the immunodominant CD4 T cell epitope encoded by ova₃₂₃₋₃₃₉. This strain is resistant to streptomycin (Strep). The suicide-counterselection vector pLR16-PheS* was a gift from Anat Herskovits (Addgene plasmid #98783; <http://n2t.net/addgene:98783>; RRID:Addgene 98783). To delete ActA or InlB, approximately 800~1000 bp fragments upstream and downstream from the deleted regions were separately amplified by PCR using Q5 polymerase (NEB) and inserted between the XhoI and BamHI sites of pLR16-pheS* using NEBuilder HiFi DNA assembly master mix following directions from the manufacturer. ActA upstream fragment primers: 5'-AGCT-GGTACCGG GCCCCCCCAACGCATGCAGTTATCCAG-3', 3'-GCTC GGCATAACTTCACGTGCAGTTT-CG-5'. ActA downstream fragment primers: 5'-CACGTGAAGTTATGCC GAGCCTACCACTAATC-3'. 3'-CGGCCGCTCTAGAACT AGTGTGCTACCATGTCTTCCGTTG-5'. InlB upstream fragment primers: 5'-AG-CTGGTACGGGGCCCC CCTGGGATTTCGCAACTAGC-3', 3'-AATTAGCTGCCT TCCTTCTGGGTTG-TG-5', InlB downstream fragment primers: 5'-AAGAAGGAAGGCAGCTAATTAAAG GGCAC-3', 3'-CGGCCGCTCTAGAACTAGTGTG ACCAGTTACTAAATAAG-5'. The resulting plasmids pLR16-ΔActA and pLR16-ΔInlB were confirmed with restriction digestion and sequencing. Deletions were achieved according to the published protocol.³⁵ Briefly, the plasmids were transformed into the conjugation donor strain Sm10pir, then transferred into the recipient InLA^M *Lm*-ova strain or its derivatives by conjugation.⁶⁷ Transconjugants were selected by incubation on Brain Heart Infusion (BHI) agar plates containing 200 μg/mL Strep and 10 μg/mL chloramphenicol (Cm) at 37°C for 24 hours. Clones were inoculated into BHI broth supplemented with Cm and grown at 41°C with agitation overnight. Bacteria from this culture were plated on BHI agar containing Cm at 41°C until large colonies were formed. Colonies were inoculated in BHI broth and cultured at 30°C overnight. The culture was serially diluted and plated on BHI agar supplemented with 18 mM p-Cl-phe (Sigma-Aldrich, C6506-25G) and incubated at 37°C

overnight.⁶⁸ Single colonies that grew up were verified to be Cm-sensitive and contain the desired mutation using detection primers by colony PCR (online supplemental Figure S1B). ΔActA detection primers: 5'- ATGCGT-GCGATGATGGTAGT-3', 3'- CGGCCGCTCTAGAACT-AGTGTGCTACCATGTCTCCGTTG-5'. ΔInlB detection primers: 5'- GCCT-ACAAACAAATAACGGCG-3', 3'- TCCGTTTCAGCGAATCAGT-5'.

Mice and oral immunization

Female C57Bl/6J (B6) and C57Bl/6-Tg (CAG-EGFP)131Osb/LeySopJ (B6-EGFP) mice were purchased from the Jackson Laboratory and used between 8 and 16 weeks of age. CD45.1⁺ OT-I *Rag1*^{-/-} transgenic mice were bred in-house. Mice were housed under specific-pathogen-free conditions. All procedures were carried out in accordance with National Institutes of Health guidelines and approved by the Stony Brook University Institutional Animal Care and Use Committee and Cold Spring Harbor Laboratory Institutional Animal Care and Use Committee.

Prior to infection, mice were deprived of food and water for up to 6 hours. Foodborne infection was performed by providing~1 cm³ piece of bread inoculated with designated *Lm* strains and doses in PBS to individually housed mice.⁶⁵

Enumerating *Lm* burden

MLN, spleen, liver, pancreas and brain were processed in 1% saponin. Small intestinal and colorectal contents were flushed using RPMI containing 5% heat-inactivated bovine serum. Intestinal tissues were homogenized using a GentleMACS (Miltenyi Biotec) and lysed with 1% saponin. Cell suspensions were incubated at 4°C for 1 hour prior to plating onto BHI agar plates containing 200 µg/mL streptomycin. Plates were incubated at 37°C for enumeration 24–48 hours later.

Adoptive transfers

Spleens were isolated from CD45.1⁺ OT-I *Rag1*^{-/-} mice and processed into single-cell suspensions. 1×10⁴ cells were intravenously transferred into naïve B6 mice (CD45.2⁺) 1 day prior to foodborne infection.

Flow cytometry

Spleen and MLN were processed through 70 µm cell strainers. siLP, siIEL, cLP, and cIEL were processed as previously described.^{69 70} Tumors were dissected and minced in digestion buffer containing 500 U/mL Collagenase Type I (Gibco) and 20 µg/mL DNase I (Roche), then digested in a shaker at 1,000 rpm and 37°C for 40 min. Tumors were then dissociated with a gentleMACS Dissociator (Miltenyi Biotec) using m_impTumor_01.01 and filtered through 70 µm cell strainers. Blood samples were processed with RBC Lysis buffer (BioLegend) prior to staining. Cells were stained with fluorochrome-conjugated antibodies in the presence of Fc-block for 20 min at 4°C in the dark (online supplemental table S1). Panels containing H2-K^b ova-tetramers were stained for

1 hour in the dark at ambient temperature. Cells were fixed with 2% paraformaldehyde for 20 min at 4°C in the dark. Data were acquired on a LSRFortessa (BD Biosciences) or Cytek Aurora and analyzed with FlowJo software (Tree Star). A generic gating strategy is shown (online supplemental figure S2).

T cell stimulations

Cells isolated from spleen, MLN, and siIEL were stimulated for 5 hours as described previously.⁷¹ Briefly, cells were stimulated with 2 µL/mL of BD leukocyte activation cocktail (BD Biosciences) or with 1 µg/mL of the ova SIINFEKL epitope in the presence of 1 µg/mL BD GolgiPlug (BD Biosciences). Unstimulated cells were used as controls. Following stimulation, cells were stained with surface antibodies for 20 min in the dark at 4°C. Cells were then fixed and permeabilized with BD Cytofix/Cytoperm kit (BD Biosciences) prior to intracellular staining with anti-IFNγ (XMG1.2) or anti-TNF (MP6-XT22). Data were acquired on a Cytek Aurora and analyzed with FlowJo software.

Mouse intestinal organoid culture

Lo^{SIIN}-GFP AKPS (*Apc* KO; *Kras* G12D; *Trp53* KO; *Smad4* KO)³⁰ were embedded in Matrigel (Corning) and cultured with minimal media (Advanced DMEM F-12 (Gibco) supplemented with N-2 (Thermo Fisher), B-27 (Thermo Fisher), and Primocin (InvivoGen). Organoids were split using TrypLE Express enzyme (Gibco) every 3 days as previously described.³⁹

Endoscopy-guided orthotopic tumor transplantation and murine colonoscopy

Orthotopic injections of MC38-ova cells were performed as described previously.³⁸ Briefly, cell lines were split 2 days prior to the injection day. On the day of injection, cells at 80–90% confluence were harvested by TrypLE Express enzyme (Gibco) following the manufacturer's instruction. Cells were washed with PBS and counted. 1.0×10⁶ cells in 100 µL were injected into the colon submucosa of B6 mice by optical colonoscopy using a Hamilton syringe (7656-1) and a custom 33G needle (Hamilton, custom made similar to 7803-05, 16", Pt 4, Deg 12). Successful injections were confirmed by observing large bubbles in the colon mucosa. Optical colonoscopy was performed using a Karl Storz figure 1 HD Camera System, figure 1 HUB CCU, 175-Watt Xenon Light Source, and Richard Wolf 1.9 mm/9.5 Fr Integrated Telescope (part number 8626.431) pre and post treatments for *in vivo* tumor index assessment. For orthotopic injections of lo^{SIIN} AKPS organoids,^{38 72} organoids were split 3 days prior to the day of injection. On the day of injection, Matrigel was dissolved in Cell Recovery Solution (Corning) following the manufacturer's protocol. A small portion of the organoids was fully digested by TrypLE Express enzyme for counting. Tumor cells were resuspended in PBS+10% Matrigel. 0.5–1×10⁶ cell-worth of tumors in 100 µL were injected into the colon sub-mucosa of B6-EGFP mice as above.

The tumor index was calculated as tumor area divided by lumen area \times 100.⁷³ Tumor sizes were also quantified ex vivo by a caliper and according to the formula: size (mm³)=length (mm) \times width (mm)²/2 post harvesting.⁷⁴

Immunotherapy of tumor-bearing mice

Lo^{SIIN} AKPS organoids were implanted in mouse colon as described above, and the presence of tumor was confirmed on day 7. On 21 days postimplantation, mice were intraperitoneally injected with anti-PD-1 antibody (BioXcell, BE0146; 200 μ g per dose) and anti-CTLA-4 antibody (BioXcell, BE0131; 200 μ g initial dose and following doses of 100 μ g) every other day for 2 weeks.

Statistical analysis

Statistical analyses were performed in Prism (GraphPad Software) as indicated within figure legends. Data comparing two groups were analyzed using a student's t-test. Analysis of bacterial burden was assessed by a Mann-Whitney test. Data comparing three or more groups were analyzed using a one-way analysis of variance with a post hoc Tukey's multiple comparisons test, except for online supplemental figure S8 B and C which used a Kruskal-Wallis test with a post hoc Dunn's multiple comparisons test. *p \leq 0.05; **p \leq 0.01; ***p \leq 0.001; ****p \leq 0.0001.

Acknowledgements We acknowledge the support of the NIH Tetramer Core Facility for providing MHC I monomers. Experimental model depictions were created with BioRender.

Contributors BS and SB directed and designed the study. XL, YY, CC, ZQ, YZ, TC, XL, RY, KAO, and MB performed the experiments. BS, PW, and SB provided resources. XL, YY, and CC analyzed the data. XL and YY wrote the manuscript. BS and SB edited the manuscript. BS is the guarantor.

Funding This study was supported by Department of Defense grant W81XWH-18-1-0217 (B. S. Sheridan), NIH/NIAID grant R01AI172919 (B. S. Sheridan), the G Harold and Leila Y Mathers Charitable Foundation (B. S. Sheridan) and Research Foundation for the State University of New York and Stony Brook University (B. S. Sheridan). S. Beyaz was supported by Oliver S and Jennie R Donaldson Charitable Trust, the G Harold and Leila Y Mathers Charitable Foundation, the Mark Foundation for Cancer Research (20-028-EDV) and STARR Cancer Consortium (I13-0052). Y. Yu was supported by a Scholars in Biomedical Sciences Training Program (T32 GM148331).

Competing interests No, there are no competing interests.

Patient consent for publication Not applicable.

Ethics approval Not applicable.

Provenance and peer review Not commissioned; externally peer reviewed.

Data availability statement Data are available upon reasonable request.

Supplemental material This content has been supplied by the author(s). It has not been vetted by BMJ Publishing Group Limited (BMJ) and may not have been peer-reviewed. Any opinions or recommendations discussed are solely those of the author(s) and are not endorsed by BMJ. BMJ disclaims all liability and responsibility arising from any reliance placed on the content. Where the content includes any translated material, BMJ does not warrant the accuracy and reliability of the translations (including but not limited to local regulations, clinical guidelines, terminology, drug names and drug dosages), and is not responsible for any error and/or omissions arising from translation and adaptation or otherwise.

Open access This is an open access article distributed in accordance with the Creative Commons Attribution Non Commercial (CC BY-NC 4.0) license, which permits others to distribute, remix, adapt, build upon this work non-commercially, and license their derivative works on different terms, provided the original work is properly cited, appropriate credit is given, any changes made indicated, and the use is non-commercial. See <https://creativecommons.org/licenses/by-nc/4.0/>.

ORCID iD

Peter M K Westcott <https://orcid.org/0000-0001-9436-4857>

Brian S Sheridan <https://orcid.org/0000-0002-3299-5888>

REFERENCES

- 1 Siegel RL, Giaquinto AN, Jemal A. Cancer statistics, 2024. *CA Cancer J Clin* 2024;74:12–49.
- 2 Bilotta MT, Antignani A, Fitzgerald DJ. Managing the TME to improve the efficacy of cancer therapy. *Front Immunol* 2022;13:954992.
- 3 Le DT, Wang-Gillam A, Picozzi V, et al. Safety and survival with GVAX pancreas prime and Listeria Monocytogenes-expressing mesothelin (CRS-207) boost vaccines for metastatic pancreatic cancer. *J Clin Oncol* 2015;33:1325–33.
- 4 Wei SC, Levine JH, Cogdill AP, et al. Distinct Cellular Mechanisms Underlie Anti-CTLA-4 and Anti-PD-1 Checkpoint Blockade. *Cell* 2017;170:1120–33.
- 5 Rojas LA, Sethna Z, Soares KC, et al. Personalized RNA neoantigen vaccines stimulate T cells in pancreatic cancer. *Nature New Biol* 2023;618:144–50.
- 6 Wood LM, Paterson Y. Attenuated Listeria monocytogenes: a powerful and versatile vector for the future of tumor immunotherapy. *Front Cell Infect Microbiol* 2014;4:51.
- 7 Pillich H, Chakraborty T, Mraheil MA. Cell-autonomous responses in Listeria monocytogenes infection. *Future Microbiol* 2015;10:583–97.
- 8 Shrimali R, Ahmad S, Berrong Z, et al. Agonist anti-GITR antibody significantly enhances the therapeutic efficacy of Listeria monocytogenes-based immunotherapy. *J Immunother Cancer* 2017;5:64.
- 9 Lizotte PH, Baird JR, Stevens CA, et al. Attenuated *Listeria monocytogenes* reprograms M2-polarized tumor-associated macrophages in ovarian cancer leading to iNOS-mediated tumor cell lysis. *Oncoimmunology* 2014;3:e28926.
- 10 Jahangir A, Chandra D, Quispe-Tintaya W, et al. Immunotherapy with Listeria reduces metastatic breast cancer in young and old mice through different mechanisms. *Oncoimmunology* 2017;6:e1342025.
- 11 Le DT, Brockstedt DG, Nir-Paz R, et al. A live-attenuated Listeria vaccine (ANZ-100) and a live-attenuated Listeria vaccine expressing mesothelin (CRS-207) for advanced cancers: phase I studies of safety and immune induction. *Clin Cancer Res* 2012;18:858–68.
- 12 Hassan R, Alley E, Kindler H, et al. Clinical Response of Live-Attenuated, *Listeria monocytogenes* Expressing Mesothelin (CRS-207) with Chemotherapy in Patients with Malignant Pleural Mesothelioma. *Clin Cancer Res* 2019;25:5787–98.
- 13 Le DT, Picozzi VJ, Ko AH, et al. Results from a Phase IIb, Randomized, Multicenter Study of GVAX Pancreas and CRS-207 Compared with Chemotherapy in Adults with Previously Treated Metastatic Pancreatic Adenocarcinoma (ECLIPSE Study). *Clin Cancer Res* 2019;25:5493–502.
- 14 Tsujikawa T, Crocenzi T, Durham JN, et al. Evaluation of Cyclophosphamide/GVAX Pancreas Followed by Listeria-Mesothelin (CRS-207) with or without Nivolumab in Patients with Pancreatic Cancer. *Clin Cancer Res* 2020;26:3578–88.
- 15 Braun DA, Wu CJ. Tumor-Infiltrating T Cells - A Portrait. *N Engl J Med* 2022;386:992–4.
- 16 Gooden MJM, de Bock GH, Leffers N, et al. The prognostic influence of tumour-infiltrating lymphocytes in cancer: a systematic review with meta-analysis. *Br J Cancer* 2011;105:93–103.
- 17 Pagès F, Kirilovsky A, Mlecnik B, et al. In situ cytotoxic and memory T cells predict outcome in patients with early-stage colorectal cancer. *J Clin Oncol* 2009;27:5944–51.
- 18 Pagès F, Galon J, Dieu-Nosjean M-C, et al. Immune infiltration in human tumors: a prognostic factor that should not be ignored. *Oncogene* 2010;29:1093–102.
- 19 Mackay LK, Rahimpour A, Ma JZ, et al. The developmental pathway for CD103 $+$ /CD8 $+$ tissue-resident memory T cells of skin. *Nat Immunol* 2013;14:1294–301.
- 20 Gourley TS, Wherry EJ, Masopust D, et al. Generation and maintenance of immunological memory. *Semin Immunol* 2004;16:323–33.
- 21 Sheridan BS, Pham Q-M, Lee Y-T, et al. Oral infection drives a distinct population of intestinal resident memory CD8 $+$ T cells with enhanced protective function. *Immunity* 2014;40:747–57.
- 22 Schenkel JM, Fraser KA, Beura LK, et al. T cell memory. Resident memory CD8 T cells trigger protective innate and adaptive immune responses. *Science* 2014;346:98–101.
- 23 Gavil NV, Scott MC, Weyu E, et al. Chronic antigen in solid tumors drives a distinct program of T cell residence. *Sci Immunol* 2023;8:eadd5976.

24 Ganesan A-P, Clarke J, Wood O, et al. Tissue-resident memory features are linked to the magnitude of cytotoxic T cell responses in human lung cancer. *Nat Immunol* 2017;18:940–50.

25 Malik BT, Byrne KT, Vella JL, et al. Resident memory T cells in the skin mediate durable immunity to melanoma. *Sci Immunol* 2017;2:eaam6346.

26 Nizard M, Roussel H, Diniz MO, et al. Induction of resident memory T cells enhances the efficacy of cancer vaccine. *Nat Commun* 2017;8:15221.

27 Johnson PV, Blair BM, Zeller S, et al. Attenuated Listeria monocytogenes vaccine vectors expressing influenza A nucleoprotein: preclinical evaluation and oral inoculation of volunteers. *Microbiol Immunol* 2011;55:304–17.

28 Wollert T, Pasche B, Rochon M, et al. Extending the host range of Listeria monocytogenes by rational protein design. *Cell* 2007;129:891–902.

29 Lecuit M, Dramsi S, Gottardi C, et al. A single amino acid in E-cadherin responsible for host specificity towards the human pathogen Listeria monocytogenes. *EMBO J* 1999;18:3956–63.

30 Westcott PMK, Sacks NJ, Schenkel JM, et al. Low neoantigen expression and poor T-cell priming underlie early immune escape in colorectal cancer. *Nat Cancer* 2021;2:1071–85.

31 Qiu Z, Khairallah C, Chu TH, et al. Retinoic acid signaling during priming licenses intestinal CD103+ CD8 TRM cell differentiation. *J Exp Med* 2023;220:e20210923.

32 Tilney LG, Portnoy DA. Actin filaments and the growth, movement, and spread of the intracellular bacterial parasite, Listeria monocytogenes. *J Cell Biol* 1989;109:1597–608.

33 Gaillard JL, Berche P, Frehel C, et al. Entry of L. monocytogenes into cells is mediated by internalin, a repeat protein reminiscent of surface antigens from gram-positive cocci. *Cell* 1991;65:1127–41.

34 Pentecost M, Kumaran J, Ghosh P, et al. Listeria monocytogenes internalin B activates junctional endocytosis to accelerate intestinal invasion. *PLoS Pathog* 2010;6:e1000900.

35 Argov T, Rabinovich L, Sigal N, et al. An Effective Counterselection System for Listeria monocytogenes and Its Use To Characterize the Monocin Genomic Region of Strain 10403S. *Appl Environ Microbiol* 2017;83:e02927–16.

36 Lim JY, Brockstedt DG, Lord EM, et al. Radiation therapy combined with *Listeria monocytogenes*-based cancer vaccine synergize to enhance tumor control in the B16 melanoma model. *Oncioimmunology* 2014;3:e29028.

37 Plumlee CR, Obar JJ, Colpitts SL, et al. Early Effector CD8 T Cells Display Plasticity in Populating the Short-Lived Effector and Memory-Precursor Pools Following Bacterial or Viral Infection. *Sci Rep* 2015;5:12264.

38 Beyaz S, Mana MD, Roper J, et al. High-fat diet enhances stemness and tumorigenicity of intestinal progenitors. *Nature New Biol* 2016;531:53–8.

39 Roper J, Tammela T, Cetinbas NM, et al. In vivo genome editing and organoid transplantation models of colorectal cancer and metastasis. *Nat Biotechnol* 2017;35:569–76.

40 Qu S, Xu R, Yi G, et al. Patient-derived organoids in human cancer: a platform for fundamental research and precision medicine. *Mol Biomed* 2024;5:6.

41 Schell MJ, Yang M, Teer JK, et al. A multigene mutation classification of 468 colorectal cancers reveals a prognostic role for APC. *Nat Commun* 2016;7:11743.

42 Oladejo M, Paterson Y, Wood LM. Clinical Experience and Recent Advances in the Development of *Listeria*-Based Tumor Immunotherapies. *Front Immunol* 2021;12:642316.

43 Stein MN, Fong L, Tutron R, et al. ADXS31142 Immunotherapy ± Pembrolizumab Treatment for Metastatic Castration-Resistant Prostate Cancer: Open-Label Phase I/II KEYNOTE-046 Study. *Oncologist* 2022;27:453–61.

44 Sacco JJ, Evans M, Harrington KJ, et al. Systemic listeriosis following vaccination with the attenuated Listeria monocytogenes therapeutic vaccine, ADXS11-001. *Hum Vaccin Immunother* 2016;12:1085–6.

45 Kammoun H, Kim M, Hafner L, et al. Listeriosis, a model infection to study host-pathogen interactions in vivo. *Curr Opin Microbiol* 2022;66:11–20.

46 Imperato JN, Xu D, Romagnoli PA, et al. Mucosal CD8 T Cell Responses Are Shaped by Batf3-DC After Foodborne *Listeria monocytogenes* Infection. *Front Immunol* 2020;11:575967.

47 Travier L, Guadagnini S, Gouin E, et al. ActA promotes *Listeria monocytogenes* aggregation, intestinal colonization and carriage. *PLoS Pathog* 2013;9:e1003131.

48 Liu D, Bai X, Helmkick HDB, et al. Cell-surface anchoring of Listeria adhesion protein on L. monocytogenes is fastened by internalin B for pathogenesis. *Cell Rep* 2023;42:112515.

49 Labani-Motlagh A, Ashja-Mahdavi M, Loskog A. The Tumor Microenvironment: A Milieu Hindering and Obstructing Antitumor Immune Responses. *Front Immunol* 2020;11:940.

50 Dolina JS, Van Braeckel-Budimir N, Thomas GD, et al. CD8+ T Cell Exhaustion in Cancer. *Front Immunol* 2021;12:715234.

51 Baharom F, Ramirez-Valdez RA, Tobin KKS, et al. Intravenous nanoparticle vaccination generates stem-like TCF1+ neantigen-specific CD8+ T cells. *Nat Immunol* 2021;22:41–52.

52 Reina-Campos M, Monell A, Ferry A, et al. Tissue-resident memory CD8 T cell diversity is spatiotemporally imprinted. *Nature New Biol* 2025;639:483–92.

53 Johnson LE, Brockstedt D, Leong M, et al. Heterologous vaccination targeting prostatic acid phosphatase (PAP) using DNA and *Listeria* vaccines elicits superior anti-tumor immunity dependent on CD4+ T cells elicited by DNA priming. *Oncioimmunology* 2018;7:e1456603.

54 Lippman SM, Hawk ET. Cancer prevention: from 1727 to milestones of the past 100 years. *Cancer Res* 2009;69:5269–84.

55 Livingston NK, Hickey JW, Sim H, et al. In Vivo Stimulation of Therapeutic Antigen-Specific T Cells in an Artificial Lymph Node Matrix. *Adv Mater* 2024;36:e2310043.

56 Aurisicchio L, Salvatori E, Lione L, et al. Poly-specific neoantigen-targeted cancer vaccines delay patient derived tumor growth. *J Exp Clin Cancer Res* 2019;38:78.

57 von Knebel Doeberitz M, Kloos M. Towards a vaccine to prevent cancer in Lynch syndrome patients. *Fam Cancer* 2013;12:307–12.

58 Pearlman R, Frankel WL, Swanson B, et al. Prevalence and Spectrum of Germline Cancer Susceptibility Gene Mutations Among Patients With Early-Onset Colorectal Cancer. *JAMA Oncol* 2017;3:464–71.

59 Kalbasi A, Ribas A. Tumour-intrinsic resistance to immune checkpoint blockade. *Nat Rev Immunol* 2020;20:25–39.

60 Alexandrov LB, Nik-Zainal S, Wedge DC, et al. Signatures of mutational processes in human cancer. *Nature New Biol* 2013;500:415–21.

61 Le DT, Uram JN, Wang H, et al. PD-1 Blockade in Tumors with Mismatch-Repair Deficiency. *N Engl J Med* 2015;372:2509–20.

62 Hamon MA, Ribet D, Stavru F, et al. Listeriolysin O: the Swiss army knife of Listeria. *Trends Microbiol* 2012;20:360–8.

63 van der Burg SH. Correlates of immune and clinical activity of novel cancer vaccines. *Semin Immunol* 2018;39:119–36.

64 Melief CJM, Welters MJP, Vergote I, et al. Strong vaccine responses during chemotherapy are associated with prolonged cancer survival. *Sci Transl Med* 2020;12.

65 Plumlee CR, Sheridan BS, Cicek BB, et al. Environmental cues dictate the fate of individual CD8+ T cells responding to infection. *Immunity* 2013;39:347–56.

66 Xayaratth B, Marquis H, Port GC, et al. Listeria monocytogenes CtaP is a multifunctional cysteine transport-associated protein required for bacterial pathogenesis. *Mol Microbiol* 2009;74:956–73.

67 Trieu-Cuot P, Derlot E, Courvalin P. Enhanced conjugative transfer of plasmid DNA from *Escherichia coli* to *Staphylococcus aureus* and *Listeria monocytogenes*. *FEMS Microbiol Lett* 1993;109:19–23.

68 Ji X, Lu P, van der Veen S. Development of a dual-antimicrobial counterselection method for markerless genetic engineering of bacterial genomes. *Appl Microbiol Biotechnol* 2019;103:1465–74.

69 Sheridan BS, Lefrançois L. Isolation of mouse lymphocytes from small intestine tissues. *Curr Protoc Immunol* 2012;3.

70 Qiu Z, Sheridan BS. Isolating Lymphocytes from the Mouse Small Intestinal Immune System. *J Vis Exp* 2018;2018:57281:132.

71 Chu TH, Qiu Z, Sheridan BS. The use of foodborne infection to evaluate bacterial pathogenesis and host response. *Methods Cell Biol* 2022;168:299–314.

72 Roper J, Tammela T, Akkad A, et al. Colonoscopy-based colorectal cancer modeling in mice with CRISPR-Cas9 genome editing and organoid transplantation. *Nat Protoc* 2018;13:217–34.

73 Roper J, Richardson MP, Wang WV, et al. The dual PI3K/mTOR inhibitor NVP-BEZ235 induces tumor regression in a genetically engineered mouse model of PIK3CA wild-type colorectal cancer. *PLoS One* 2011;6:e25132.

74 Zhen Z, Tang W, Chuang Y-J, et al. Tumor vasculature targeted photodynamic therapy for enhanced delivery of nanoparticles. *ACS Nano* 2014;8:6004–13.